# Simulation of laminar flame propagation in a multicomponent droplet stream

A. Bruyat*, C. Laurent, O. Rouzaud, G. Lavergne
ONERA-The French Aerospace Lab, F31055 Toulouse

**Abstract**

To predict alternative fuels performances and the flame behavior during the ignition process of a combustion chamber, a multicomponent evaporation model was implemented into the lagrangian solver of ONERA's CFD code CEDRE. Several chemical components are now considered in the droplets, and the vaporization process is sequential. The present study aims at testing the droplet composition effect on spray combustion. The academic case of a 1D laminar flame propagating along a droplet stream is investigated. The first parametric study deals with n-decane droplets and the results are compared to the equivalent gaseous flame configuration in order to understand vaporization effects. A reduced chemical scheme is considered for which Arrhenius preexponential factor is tabulated versus the equivalence ratio. Computations are performed for droplets composed with n-decane and n-hexadecane to stress how component volatilities alter flame behavior. As components are both n-alcanes, n-decane and n-hexadecane are supposed to have the same chemistry mechanism. The objective is to investigate sequential vaporization effect on flame propagation only. The modified parameters are the droplets composition, the droplets initial diameter, and the total equivalence ratio. Results on the flame speed, its temperature and its thickness are analysed.

## Nomenclature

**Latin Letters**

| | |
|---|---|
| A | Pre-exponential factor (SI) |
| $a_k$ | Reaction exponents (-) |
| d | diameter ($\mu$m) |
| Ea | Activation energy (cal/mol) |
| $M_k$ | Molecular weight (kg·m$^{-3}$) |
| $m_k$ | Number of C atoms (-) |
| $n_k$ | Number of H atoms (-) |
| P | Pressure (Pa) |
| $s_L$ | Flame speed (m·s$^{-1}$) |
| T | Temperature (K) |
| $X_k$ | mole fraction (-) |
| $Y_k$ | gaseous mass fraction (-) |

**Greek Letters**

| | |
|---|---|
| 1 | State in fresh gases |
| 2 | State in burnt gases |
| F | Fuel |
| g | gas phase |
| 1 | liquid phase |
| Ox | Oxidizer |

**Subscripts**

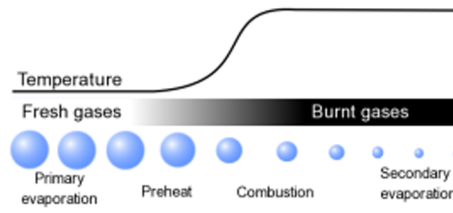| | |
|---|---|
| $\alpha$ | Volume fraction (-) |
| $\phi$ | Equivalence ratio (-) |
| $\rho$ | density (kg·m$^{-3}$) |
| $\dot{\omega}_k$ | reaction rate (kg·m$^{-3}$·s$^{-1}$) |

## Introduction

This work is a preliminary step to understand and evaluate the outcomes of multicomponent droplet composition on two-phase flow combustion phenomena such as ignition, extinction and flame propagation. The paper lays emphasis on flame propagation. Taking into account the fuel composition becomes a major feature with the introduction of alternative fuels to assess their behaviors with respect to JET A1. Indeed when droplets are multicomponent, the vaporization process is sequential and may lead to different flame spray structures. To understand these phenomena, an academic case is investigated: the propagation of a laminar flame through a 1D droplet stream. Droplets may be vaporized before reaching the flame front, or, depending on various parameters, may keep on vaporizing in the burnt gases. Fig 1 describes the case of an heterogeneous flame.

This paper presents two parametric studies dealing with a 1D laminar flame propagating through a two-phase flow. The first one is devoted to the monocomponent case and set comparisons with gaseous flame in order to underline two-phase flow effects. Then, the case of bicomponent droplets is investigated to analyse droplet composition effect on flame behavior. Parameters modified in the monocomponent case are the droplet size and

---

∗. Corresponding author: anne.bruyat@onera.fr

**Figure 1.** Laminar flame through a droplet stream

the total equivalence ratio. In the multicomponent case, the composition is also modified but the total equivalence ratio is fixed and is equal to 0.82.

Simulations are performed with CEDRE, the multiphysic ONERA CFD code [1] [2]. Two solvers are used: CHARME, the reactive eulerian gaseous solver and SPARTE, the lagrangian solver for the dispersed phase. The gaseous phase is solved using a laminar Navier-Stokes approach and an Arrhenius model for the combustion. The gas phase is composed with CO, $CO_2$, $H_2O$, $O_2$, $N_2$ and fuel vapor. The fuel vapor is a surrogate component of kerosene, $C_{10}H_{20}$, that will be improperly called *n-decane* in this paper. Its properties are described by Franzelli [3].

The fuel vapor is produced by droplet evaporation which is modeled in the lagrangian solver SPARTE. This solver is coupled with the gaseous solver CHARME at each time step using a two-way coupling approach. The model used for droplet drag coefficient in SPARTE solver to compute droplets trajectories is the Shiller and Neumann correlation. The droplet heating is solved using the infinite conduction model and evaporation uses a model based on the Sirignano's approach for multicomponent droplets [4]. Convective effects are taken into account using Ranz-Marshall correlations , and the blowing of the droplet boundary layer due to evaporation (Stefan flow) is modeled using the Abramzon and Sirignano approach [5]. The gaseous diffusion coefficient ensures the Lewis number equals unity.

Concerning the numerical parameters, the time step used in both solvers is $\Delta t = 10^{-6}$ s. The domain is 0.02 m long. The mesh is composed with 400 cells ($\Delta x = 0.510^{-4}$ m) in order to ensure the flame front resolution. For a given total equivalence ratio, the number of injected droplets depends on the droplet diameter. At the entrance, the fresh gases are saturated.

The definitions connected with the study of the flame propagation are given below.

From the gaseous flame speed given in the 1D case [7], Boileau [8] demonstrated the expression for the flame speed in two-phase flow (eq 1) for monocomponent droplets, which can be easily extended to the multicomponent case.

$$s_L = \frac{\int_{-\infty}^{+\infty} \dot{\omega}_F dx}{\rho_1^{gas} \left( Y_{F2} - Y_{F1} \right) + \rho_{l1} \alpha_{l1} \left( Y_{F2} - 1 \right)} \tag{1}$$

where $s$ is the stoichiometric ratio.

The total equivalence ratio is defined as the sum of the gaseous and liquid equivalence ratios:

$$\Phi_{tot} = \Phi_g + \Phi_l = s \left( \frac{Y_{F,g}}{Y_{Ox,g}} + \frac{\alpha_l \rho_l}{\alpha_g \rho_g Y_{Ox,g}} \right) \tag{2}$$

where $s$ is the mass stoechiometric ratio $s = \left( \frac{Y_{Ox}}{Y_F} \right)_{st}$.

The effective equivalence ratio is the gaseous equivalence ratio based on the mass fraction of the carbon element [9] [10], where the heat release is maximal.

$$\Phi_{eff} = \Phi_{g,\dot{w}_{T,max}} \tag{3}$$

**Laminar flame propagation in a monocomponent droplet stream**

*Literature review of numerical studies*

Laminar flame propagation in a kerosene droplet stream has already been numerically studied by Boileau [8] and Neophytou [10]. Neophytou [10] studied laminar flames in monocomponent droplet mists for n-decane and n-heptane droplets, with a detailed chemistry, under atmospheric and relight conditions. The gas is not saturated,

so the effect of the primary evaporation zone is also studied. Author compared results for n-heptane and n-decane. It was pointed out that, for lean conditions, the reduction of the flame speed with increasing diameter is more important in the case of the less volatile component, n-decane. The numerical study was in agreement with Ballal and Lefebvre results [12], showing that in rich conditions an optimal diameter exists such that the flame speed is maximal. Finally, Neophytou *et al.* investigate the effective equivalent ratio. No complete correlation was found with the pure gaseous case. It may be explained by the pyrolisis of the fuel in rich sprays with large droplets.

Boileau [8] studied the combustion of JP-16 droplets, with a one-step chemical scheme, and Senoner [11] studied combustion of kerosene monocomponent droplets. The gaseous phase is initially saturated with the fuel. New adimensionnalized numbers are defined to analyse the evaporation behavior of droplets through the flame front. The predominant effect on the flame comes from the two-phase flow rather than the kinetic. The flame speed evolution is slower with the total equivalence ratio in a droplet burning stream than in the gaseous case. Finally, the theoretical formula for the flame speed, by Ballal and Lefebvre [12], valid in the case of a lean mixture, is respected in the case of large enough droplets. For a monodisperse and monocomponent spray, the formula is:

$$s_L^{diph} = \alpha_g \left[ \frac{(1-\Omega)\rho_{liq}d^2}{8\rho_{gas}ln(1+B_M)} + \left( \frac{\alpha_g}{s_L^{gas}} \right)^2 \right]^{-0.5} \tag{4}$$

where $\Omega$ is the fraction of total fuel in form of vapor, $\alpha_g$ is the thermal diffusivity of the gas, and $B_M$ is the Spalding number to caracterize mass transfer.

The simple kinetics results should be compared to the detailed chemistry study in order to know the limitations of using a global chemical scheme.

### Simulations using ONERA CFD code CEDRE

#### Initial and boundary conditions

Numerical simulations of flame propagation in a monocomponent droplet stream were conducted with n-decane droplets. The gas is saturated under atmospheric conditions with the pseudocomponent $C_{10}H_{20}$ introduced by Franzelli [3] to represent kerosene. The liquid properties of the droplets are surrogate of kerosene liquid properties. The initial droplet diameter is given by calculations taking into account the saturation process (for example, it is improperly written $d_0 = 25\,\mu m$ instead of $d_0 = 24.86\,\mu m$). The varying parameters are the diameter ($5\,\mu m \leq d_0 \leq 100\,\mu m$) and the initial total equivalence ratio ($0.73 \leq \phi_0 \leq 1.94$). A global chemistry approach for kerosene called $2S\_KERO\_BFER$ is used [3].

The air mass flow is imposed at the inlet of the domain, and non-reflecting boundary conditions are used at the outlet.

#### Results

At the lower diameter, the flame structure is like a gaseous flame, since the droplets are evaporated before reaching the flame front. The flame becomes heterogeneous when the diameter increases, and droplets go on evaporating in the burnt gases. For the larger diameters ($d_0 = 100\,\mu m$), the fuel is consumed as soon as it is evaporated from the droplet, the flame thickness is larger and the maximum of the heat release is lower.
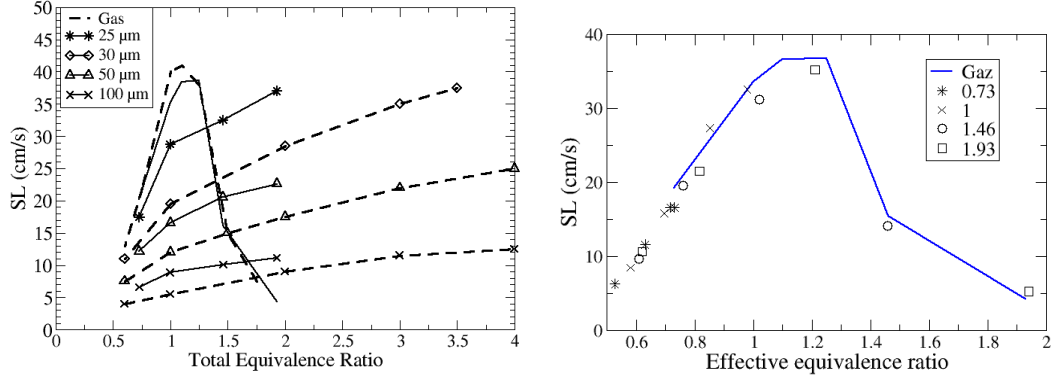
The flame speed evolution versus the total equivalence ratio, for different initial droplet diameters is plotted and compared to Neophytou results on Fig 2. For a given initial diameter, the global evolution of the flame speed is the same as Neophytou's. However the flame speed values are not equal. It can be explained by the different models chosen for the droplet heat, gaseous diffusion coefficient, and particularly for the chemistry (Neophytou used a detailed chemistry). However, the comparison with Neophytou's study validates the present approach.

Then, the flame speed versus the effective equivalence ratio is plotted on Fig 2. For a given initial ratio, the largest effective equivalent ratio belongs to small droplets ($d_0 = 5\,\mu m$), the following ones stand for droplets for which $d_0 = 25\,\mu m$, $d_0 = 50\,\mu m$ and finally $d_0 = 100\,\mu m$. Those results demonstrate that the effective equivalence ratio is a relevant parameter to fit the flame speed for two-phase flows with the gaseous flame speed.

## Laminar flame propagation in a multicomponent droplet stream

### Literature review

Yang set up experiments on the autoignition of mono and multicomponent droplets [13]. Chemical kinetic effects were investigated by comparing the autoignition of droplets composed with iso-octane and n-heptane, which have similar volatilities. Depending on the droplet diameter, the ignition delay times are reaction-controlled or evaporation-controlled. For the latter case, the droplet composition strongly affects the delay times.

**Figure 2.** Flame speed versus total equivalence ratio ($d_0 = 5\,\mu m$ follows the gas) - dashed line: Neophytou, solid line: current study ; Flame speed versus effective equivalence ratio, for different total equivalence ratio and initial diameters (5, 25, 50, 100$\mu$m)

Aggarwal used a global one-step reaction scheme described previously to investigate autoignition of multicomponent sprays by a hot wall [14] [15]. He found out that a small amount of a volatile component can improve the ignibility of a non-volatile fuel spray.
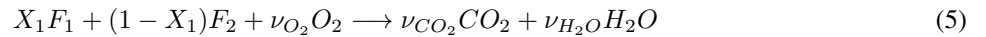
Generally, literature studies deal with multicomponent effects of the droplet composition on ignition delays while this present paper focuses on the composition effects on flame propagation.

### Kinetic models

The chemical scheme is a key-point in modelling combustion. Using a detailed chemistry is too expensive for industrial applications, thus a reduced chemical scheme is chosen.

Westbrook and Dryer proposed a two-step monocomponent chemical scheme for n-alkane enabling to reproduce the laminar flame speed and the adiabatic flame temperature for a wide range of temperature, pressure and equivalence ratio [16]. Now, the issue is to extend this reduced chemical schemes to the multicomponent fuel.

**Global chemical scheme**    Aggarwal adapted the Westbrook and Dryer chemical scheme to a multicomponent case [14]. For a bicomponent fuel composed of $F_1$ and $F_2$, it becomes:

$$X_1 F_1 + (1 - X_1)F_2 + \nu_{O_2} O_2 \longrightarrow \nu_{CO_2} CO_2 + \nu_{H_2O} H_2O \tag{5}$$

The global nondimensional reaction rate is expressed as:

$$\dot{\omega}_r = A\left([F_1] + [F_2]\right)^{a_F} [Ox]^{a_O} e^{-\frac{Ta}{T}} \tag{6}$$

Considering two fuel components identical to a classic fuel, this multicomponent approach is validated on a 1D laminar gaseous flame compared to the monocomponent case. This method has the strong advantage that the preexponential factor and then the reaction rate can be corrected with a function in the case of rich mixtures. However this method can only be applied to components with equal energy of activation, when they are from the same family (ex: n-alkanes). In case of components with very different thermophysical properties, the energy of activation of the components may not be equal. For these reasons, separate reactions for each fuel components are also investigated.

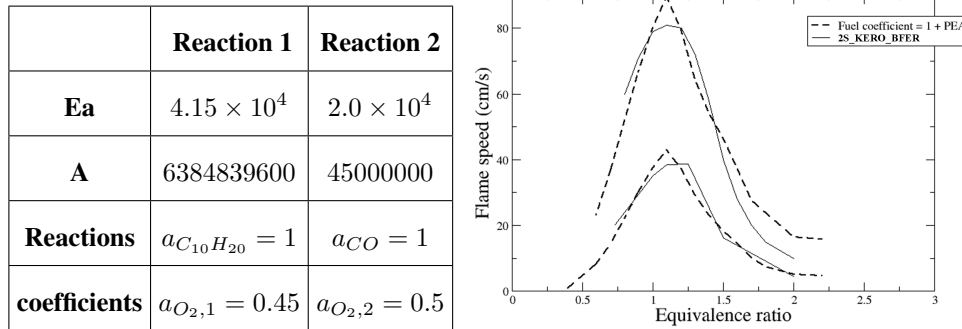**Separate component reactions**    The reactions considered are given by equations 7, for $i$ fuel components:

$$F_i + Oxidizer \Rightarrow Products_i \tag{7}$$
$$CO + 0.5O_2 \Leftrightarrow CO_2 \tag{8}$$

where the reactions rates are:

$$\dot{w}_{F_i} = A_i f_1(\phi) e^{(-Ea_i/RT)} [F_i]^{a_{F_i}} [O_2]^{a_{O_2,1}} \tag{9}$$
$$\dot{w}_{oxydation} = A_2 f_2(\phi) e^{(-Ea_2/RT)} [CO]^{a_{CO}} [O_2]^{a_{O_2,2}} \tag{10}$$

where $f_1$ and $f_2$ are corrective functions developped by Franzelli to ensure the gaseous flame speed when the mixture is rich [3].

This approach implies that the fuel reaction coefficient $a$ is equal to 1. Indeed the global reaction rate has to depend linearly on the sum of fuel concentrations to ensure the validation of a monocomponent fuel treated as a multicomponent one. The preexponential factor $A$ is consequently modified. A new kinetic scheme using $a_{Fuel} = 1$ is then obtained for the n-decane, Arrhenius coefficients being given in table 3 a) .

|  | **Reaction 1** | **Reaction 2** |
|---|---|---|
| **Ea** | $4.15 \times 10^4$ | $2.0 \times 10^4$ |
| **A** | 6384839600 | 45000000 |
| **Reactions** | $a_{C_{10}H_{20}} = 1$ | $a_{CO} = 1$ |
| **coefficients** | $a_{O_2,1} = 0.45$ | $a_{O_2,2} = 0.5$ |

**Figure 3.** a: Coefficients of the global kinetic sheme, b: Laminar flame speed versus equivalence ratio, for $T_{freshgases} = 300\ K$ and $T_{freshgases} = 473\ K$

For a monocomponent fuel composition (e.g. $i = 1$), the gaseous flame speed evolution was computed for two initial temperatures $T = 300\ K$ and $T = 473\ K$. Fig 3 shows the agreement with the $2S\_KERO\_BFER$ scheme from Franzelli [3]. However, for the multicomponent cases, the correction function can not be used when the mixture is rich since it is not a linear function. That is why only lean mixture are simulated so far.

### Simulation using CFD Onera code CEDRE

This part aims at studying the composition effect on flame propagation considering bicomponent droplets, and to compare the performances to the two multicomponent chemical schemes. The global chemical scheme is applied with coefficients and correction functions from Franzelli [3].

The two droplet components correspond to n-decane $C_{10}H_{22}$, and one of the less volatile component of kerosene: n-hexadecane $C_{16}H_{34}$. The liquid properties of the second component are taken from Reid [6]. Chemistry effects are simplified since the same kinetic scheme are considered for of each component. It means that in the gaseous phase both components have the same gaseous properties as the pseudocomponent $C_{10}H_{20}$. This assumption enables to test only bicomponent evaporation effect on flame propagation.

The flame speed of n-alkanes having more than 6 C-atoms are close. Kumar experimentally investigated the flame speed of $n - decane$ and $n - dodecane$, and found out that under the same equivalence ratio and preheat temperature, the n-decane flame speed is slightly higher (about $3\ cm/s$) than the n-dodecane flame speed [17]. Such comparison are also available from numerical studies [10]. Thus, the main consequence of this simplifying hypothesis is the overestimation of the flame speed in the case of $C_{16}H_{34}$ droplets.

The Ballal and Lefebvre [12] estimation of the flame speed 4 can be extended to the multicomponent case: the droplet mass flow rate should be defined as the sum of the mass flow rate of all components of the droplet, depending on the the Spalding number of each component.

#### Initial conditions

Gas pressure and temperature values are the same as previously. Fresh gases are saturated with both fuel components. The gaseous mass fractions are calculated from Raoult's law where the pressures of saturation are given by the Clausius-Clapeyron law. The total equivalence ratio is equal to $\phi_0 = 0.82$ and diameters are taken between $25\ \mu m$ and $100\ \mu m$. The droplet is composed of n-decane, and n-hexadecane is added $(0\ \%, 25\ \%, 50\ \%, 75\ \%, 100\ \%)$.
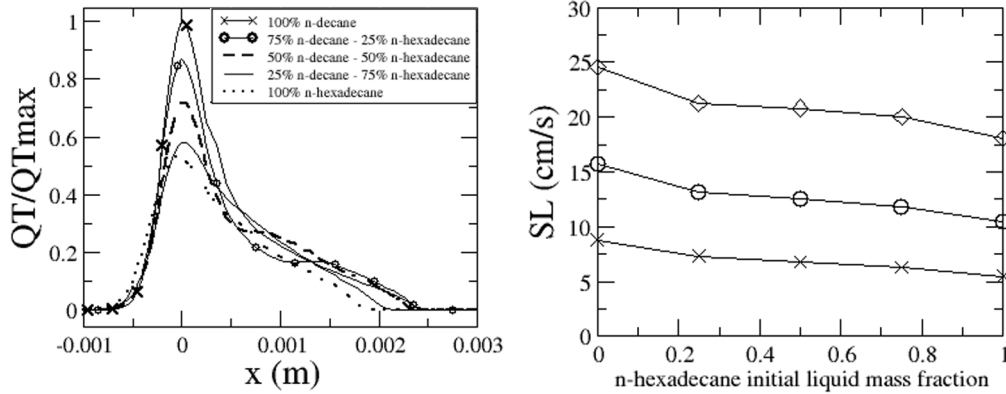
#### Multicomponent droplet effects on flame structures

Since the two chemical schemes give similar results, then only results obtained with the second approach (seperate component reactions) will be plotted.

The structure of the multicomponent two-phase flow flames is first investigated. Only the results for the

100 $\mu m$ initial diameter droplets are represented, since the multicomponent effect is more obvious.
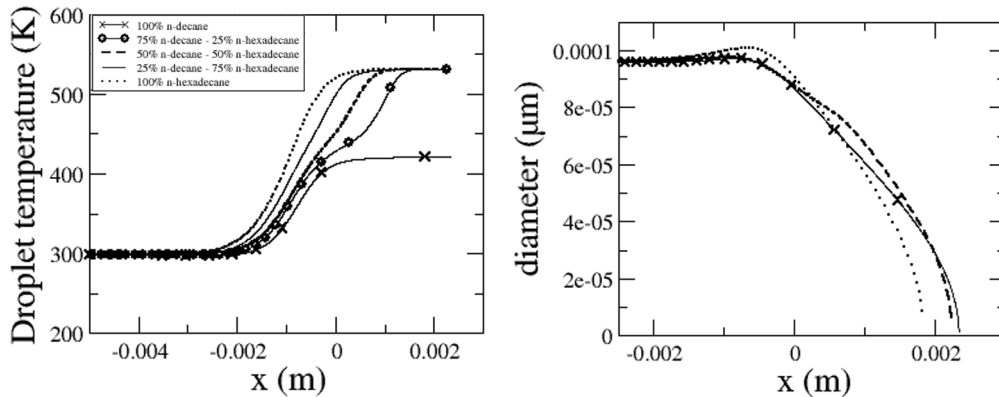
The gaseous heat release profiles are plotted for the five different tested compositions (Fig 4:a ). Profiles are affected by the multicomponent aspect since the maximum heat release decreases with addition of $C_{16}H_{34}$. For two components droplets, two maxima appear. The first peak is representative of the combustion of n-decane whereas the second one corresponds to the n-hexadecane combustion. Adding $C_{16}H_{34}$ increases the second peak intensity and decreases the distance between the two peaks. The existence of two local maxima of the heat release is significant of the existence of one flame front for each component combustion. When n-hexadecane is the major component, the small amount of n-decane enables the combustion before the n-hexadecane is vaporized.



**Figure 4.** a: Heat release profiles adimensionalized by the n-decane maximum value at $d_{ini} = 100 \ \mu m$ (abscissas shifted with respect to the maximum heat release); b: Flame speed evolution versus the initial liquid mass fraction of n-hexadecane - $\Diamond$: $d = 25 \ \mu m$, $\circ$: $d = 50 \ \mu m$, $\times$: $d = 100 \ \mu m$

Fig 4:b presents the flame speed evolution versus the addition of n-hexadecane for all initial diameters. The effect of the different volatilities of each component can be noticed: the more $C_{16}H_{34}$ is added, the slower is the flame. The flame speed for the different mixing is between the monocomponent values. This result is in good agreement with the estimation of the flame speed 4 if extended to the multicomponent case: when increasing the normal boiling temperature of the component, the Spalding number decreases according to Myers and Lefebvre [18], so adding n-hexadecane decreases the flame speed.

The behavior of the multicomponent droplet in the flame is investigated. The droplet temperature profiles show the sequential process of evaporation when a small amount of n-hexadecane is added (Fig 5).



**Figure 5.** Droplet temperature and diameter profiles through the flame at $d_{ini} = 100 \ \mu m$ (abscissas are shifted with respect to the maximum heat release)

The droplet diameter profiles are also affected by the multicomponent effect (Fig 5). Addition of n-hexadecane leads to a longer preheat, which have two effects. Firstly, the maximal droplet size increases with the n-hexadecane initial liquid mass fraction due to the higher boiling temperature value. Secondly, the pure vaporization process of droplets begins at a point where the gas temperature is higher than it is when the droplet is composed of pure n-decane. Since the gas conditions are different at this point, the pure vaporization of n-hexadecane is faster.

6

However, the total evaporation time (preheat and evaporation) is actually longer than n-decane one, as expected from the liquid properties.
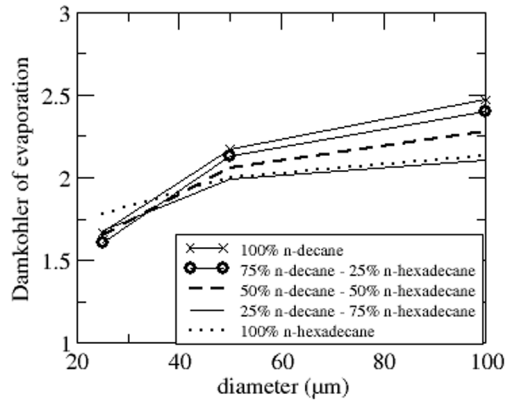
Evaporation thickness $\delta_{ev}$ and flame thickness $\delta_L$ are then investigated to characterize the flame structure. Indeed small droplets are vaporized before reaching the flame front whereas large droplets keep on vaporizing in the burnt gases. In order to study how far droplets go into burnt gases, Boileau introduced non-dimensional numbers [8], and especially the Damkohler number for evaporation $Da_{ev}$. Here the total evaporation thickness is defined as the thickness from the beginning of the preheat ($T > 304\ K$) to the end of the evaporation of the droplet:

The Damkholer number increases with the diameter (Fig 6): the evaporation thickness increases with the droplet diameter more than the flame thickness. On the other hand, the Damkohler number decreases with the addition of n-hexadecane. Consequently, the composition affects more the flame thickness than the evaporation thickness.

$$Da_{ev} = \frac{\delta_{ev}}{\delta_L}$$

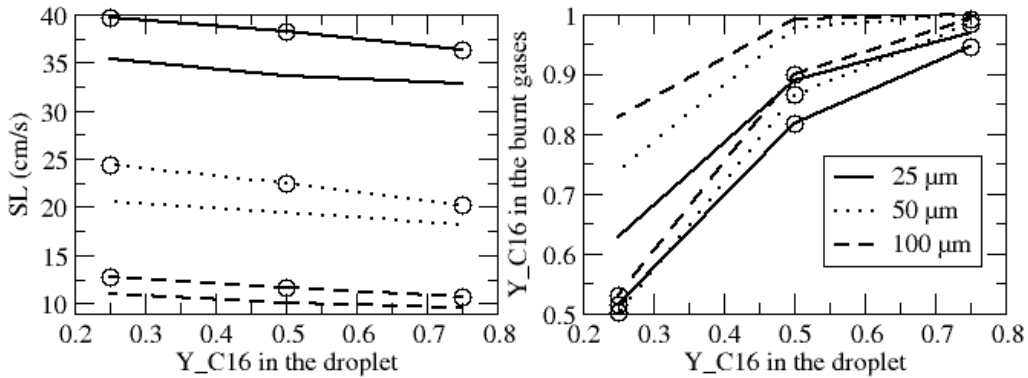where the flame thickness is given by:

$$\delta_L = \frac{T_{burntgases} - T_{freshgases}}{(gradT)_{max}}$$



**Figure 6.** Damkohler evolution versus the initial diameter

### Multicomponent approach applied to rich combustion

The global reaction scheme is applied to 1D laminar flames with a rich mixture ($\phi_0 = 1.47$ and $\phi_0 = 1.95$). The droplet diameters are $25\ \mu m$, $50\ \mu m$ and $100\ \mu m$, and the percentage of n-hexadecane in droplets varies from 25 % to 75 %. Flame speed and composition of burnt gases are investigated on Fig. 7.



**Figure 7.** Behavior of the flame in rich cases, no symbols: $\phi_0 = 1.47$, circles: $\phi_0 = 1.95$. a) Flame speed, b) Mass fraction of n-hexadecane in the burnt gases

As it does with lean combustion, the flame speed decreases when the n-hexadecane mass fraction increases since the evaporation process is longer. The mass fraction of the burnt gases show that the sequential evaporation of droplets leads to a preferencial composition of the burnt gases, which strongly depends on the total equivalence ratio $\phi_0$ and on the droplets diameter. The most volatile component is first vaporized and consumes oxydant, then the less volatile component of the droplets is more represented in the burnt gases. Given that the flame speed decreases when increasing the number of C-atoms in the n-alkane fuel, this effect is expected to be even more

important if the properties of the n-hexadecane component are taken into account.

## Conclusion

This paper aims at studying the effect of droplet composition on the flame propagation through a droplet stream.

In a first step, the approach has been validated thanks to comparisons with literature performed for monocomponent droplets. The models enable to obtain satisfactory tendencies for 1D flame propagation in two-phase flows. The evolution of the flame speed versus the total equivalence ratio is well reproduced. For a given total equivalence ratio, the droplet diameter strongly affects the flame speed: the flame speed is slower when the diameter is larger. This study was performed for diameters from 5 $\mu m$ to 100 $\mu m$ and for total equivalence ratio from 0.73 to 2. These simulations show the same behavior than in literature even if the flame speed value is slightly overestimated due to the simple chemistry used in the present study.

In a second step, flame propagation has been studied for bi-component droplet. Firstly, the study focuses only on the effects of the component volatility. Consequently, the same kinetic is used for the two components. The multicomponent evaporation model implemented in the lagrangian solver CEDRE is used. The simulations have been performed for a given total equivalence ratio and for several droplet diameters between 5 $\mu m$ and 100 $\mu m$. It appears that the flame speed decreases with the addition of n-hexadecane (one of the less volatile component of kerosene). The heat release profiles are very dissimilar between bicomponent and monocomponent cases (two maxima instead of one). The flame thickness and the evaporation Damkohler number are quite affected by the droplet composition. The structure of the flame (homogeneous or heterogeneous) depends on the droplet composition, and the global behavior (ex: flame speed) for multicomponent cases are between the monocomponent values. An investigation of the combustion of rich mixtures shows that the composition of the burnt gases are strongly affected by the multicomponent composition of the droplets. The next step will be to consider different chemical kinetics for each component. The final objective is to characterize separately evaporation and chemistry effects. This would be helpfull to understand more complex phenomena encountered in combustion chamber when alternative fuels are used.

## Acknowledgements

## References

[1] J. J. Thibert, *CFD Platforms and coupling,The ONERA Journal Aerospace Lab*, Issue 2, March 2011

[2] A. Refloch, B. Courbet, A. Murrone, P. Villedieu, C. Laurent, P. Gilbank, J. Troyes, L. Tessé, G. Chaineray, J.B. Dargaud, E. Quémerais, F. Vuillot, *CEDRE Software,The ONERA Journal Aerospace Lab*, Issue 2, March 2011

[3] B. Franzelli, E. Riber, M. Sanjosé, T. Poinsot, *Combustion and Flame*, Volume 157, Issue 7, July 2010

[4] W. A. Sirignano, *Fluid Dynamics and Transport of Droplets and Sprays, Cambridge University Press*, 1999

[5] B. Abramzon, W.A. Sirignano, *Int. J. Heat Mass Transfer 32*, 1989

[6] Reid, *The Properties of Gases and Liquids*, McGraw-Hill Book Company

[7] T. Poinsot, D. Veynante, *Theoretical and Numerical Combustion,* second ed., R.T. Edwards, 2005

[8] M. Boileau, *Simulation aux grandes échelles de l'allumage diphasique des foyers aéronautiques, Université de Toulouse, PhD Thesis*, 2007

[9] N. Bertier, L.H. Dorey, *Mécanisme réactionnel avec PEA pour la combustion du kérosène dans l'air, Rapport technique ONERA, RT 3/17454 DEFA*, December 2010

[10] A. Neophytou, E. Mastorakos, *Combustion and Flame*, Volume 156, 2009

[11] J.M. Senoner, *Simulation aux Grandes Echelles de l'écoulement diphasique dans un bruleur aéronautique par une approche Euler-Lagrange, Université de Toulouse, PhD Thesis*, 2009

[12] Ballal DR, Lefebvre AH., *Proceedings of the Combustion Institute 18*, 1981

[13] J.R. Yang, C.Y Yukao, J.J. Whang, S.C. Wong, *Combustion and Flame 123*, Issue 123, 2000

[14] S.K Aggarwal, *Combustion and Flame 76*, 1989

[15] S.K Aggarwal, *Progress in Energy Combustion Science 24*, 1998

[16] C. Westbrook, F. Dryer, *Combust. Sci. Technol. 27*, 1981

[17] K. Kumar, C. J. Sung, *Combustion and Flame 151*, 2007

[18] G. D. Myers, A.. H. Lefebvre , *Combustion and Flame 66*, 1986